



## Electrodeposition of $\text{Co}(\text{OH})_2$ Film and its Conversion into $\text{Co}_3\text{O}_4$ Film for Supercapacitors

YANHUA LI<sup>1,2,\*</sup> and QIYUAN CHEN<sup>1</sup>

<sup>1</sup>College of Chemistry and Chemical Engineering, Central South University, Changsha 410083, P.R. China

<sup>2</sup>Department of Chemical Engineering and Information Engineering, Changsha Aeronautical Vocational and Technical College, Changsha 410019, P.R. China

\*Corresponding author: Fax: +86 731 88879850; Tel: +86 731 88830827; E-mail: liyanhua12@yahoo.com.cn

(Received: 7 September 2011;

Accepted: 12 May 2012)

AJC-11481

$\text{Co}(\text{OH})_2$  film is prepared by electrodeposition and then  $\text{Co}_3\text{O}_4$  film is obtained by calcining  $\text{Co}(\text{OH})_2$  film. Capacitive properties of these films are measured. The results show that the specific capacitance of  $\text{Co}(\text{OH})_2$  film,  $\text{Co}_3\text{O}_4$  film obtained by calcining at 200 and 300 °C at the current density of 0.2 A g<sup>-1</sup> are 153.4, 150.4 and 129.1 F g<sup>-1</sup>, respectively. The specific capacitance retention ratio of three film electrodes is above 97 % at the current density range from 0.2-1.0 A g<sup>-1</sup>. The specific capacitance retention ratio of above 88 % is obtained in three film electrodes when the current density increases from 0.2-2.0 A g<sup>-1</sup>. These values are higher than those of  $\text{Co}_3\text{O}_4$  film prepared by chemical bath deposition.

**Key Words:** Supercapacitors,  $\text{Co}_3\text{O}_4$  film, Electrodeposition, Capacitive properties.

### INTRODUCTION

Supercapacitors with high power density and long cycle life have been successfully applied in energy storage fields such as backup power storage and hybrid electric vehicles. Supercapacitors can be divided into two main categories based on their energy storage mechanisms: electric double-layer capacitors and pseudo-capacitors<sup>1</sup>. Electric double-layer capacitors store energy mainly related to non-faradaic charge separation at the electrode/electrolyte interface. Energy storage of pseudo-capacitors involves faradaic redox reactions. Carbon materials such as activated carbon<sup>2</sup>, carbon aerogel<sup>3</sup> and carbon nanotubes<sup>4,5</sup> are electrode materials for electric double-layer capacitors. Whereas transition metal oxides<sup>6,7</sup>, transition metal hydroxides<sup>8,9</sup> and conductive polymers<sup>10</sup> are electrode materials for pseudo-capacitors.

$\text{Co}(\text{OH})_2$  materials have attracted great attention because of their layered structure with large interlayer spacing and their well-defined electrochemical redox activity<sup>8,11</sup>. For example,  $\text{Co}(\text{OH})_2$  can be used as additive to enhance  $\text{Ni}(\text{OH})_2$  electrode electrochemical performance<sup>12</sup>, alkaline secondary battery materials<sup>13</sup> and supercapacitor materials<sup>14</sup>. Moreover, under the conditions of thermal decomposition,  $\text{Co}(\text{OH})_2$  often serves as a precursor material of preparation of cobalt oxide<sup>15</sup>. As an important P-type semiconductor material,  $\text{Co}_3\text{O}_4$  is applied in lithium ion batteries<sup>16</sup>, supercapacitors<sup>17</sup>, magnetic materials<sup>18</sup> and electrochromic devices<sup>19</sup>. Compared with other super-

capacitor electrode materials,  $\text{Co}_3\text{O}_4$  is a promising electrode material for supercapacitor because of its high redox activity and great reversibility<sup>20</sup>. There are many methods used to obtain  $\text{Co}(\text{OH})_2$  and  $\text{Co}_3\text{O}_4$ . Each method has its own advantages and disadvantages. Different preparation methods can get different morphologies and structures of  $\text{Co}(\text{OH})_2$  and  $\text{Co}_3\text{O}_4$ .  $\text{Co}(\text{OH})_2$  and  $\text{Co}_3\text{O}_4$  with different morphologies and structures have important influence on the properties of materials. Compared with other methods, electrodeposition has a significant advantage<sup>21</sup>: weight and thickness of deposited products can be easily controlled by controlling the current, composition of electrodeposition solution and temperature. In addition, nano-sized  $\text{Co}(\text{OH})_2$  electrode and  $\text{Co}_3\text{O}_4$  electrode can be prepared directly onto the substrates by electrodeposition method, which isn't mixed with conducting agent and polytetrafluoroethylene binder during the electrode preparation process.

In previous work, a problem about  $\text{Co}_3\text{O}_4$  film prepared by a chemical bath deposition is a relative lower specific capacitance retention ratio<sup>22</sup>. To overcome this problem, in present work,  $\text{Co}(\text{OH})_2$  film was electrodeposited on Ni substrate by constant potential deposition and then  $\text{Co}_3\text{O}_4$  film was fabricated by calcining  $\text{Co}(\text{OH})_2$  film at different temperatures and their capacitive properties were studied. In addition, comparison about capacitive properties of  $\text{Co}(\text{OH})_2$  film and  $\text{Co}_3\text{O}_4$  film was also investigated.

## EXPERIMENTAL

Nickel substrate was employed as the substrate. Prior to use, the substrate was ultrasonically cleaned with alcohol and then washed with distilled water.  $\text{Co}(\text{OH})_2$  film fabricated by electrodeposition was similar to the reference<sup>23</sup>. Electrodeposition was carried out with a CHI 660B electrochemical workstation in a three-electrode cell with a Pt plate as the counter electrode, a saturated calomel electrode (SCE) as reference electrode and Ni substrate as the working electrode.  $\text{Co}(\text{OH})_2$  film was electrodeposited by applying a constant potential of  $-0.9$  V in aqueous solution  $0.025$  M  $\text{Co}(\text{NO}_3)_2$ . After electrodeposition, the film electrode was washed thoroughly with distilled water and then dried in an oven. As a result,  $\text{Co}(\text{OH})_2$  film was obtained. Finally,  $\text{Co}_3\text{O}_4$  film was obtained by calcining  $\text{Co}(\text{OH})_2$  film at  $200$  and  $300$  °C for 1 h in air, respectively. The structures and morphologies of as-obtained products were characterized by X-ray diffraction (XRD, Rigaku D/max2550VB<sup>+</sup> 18 kw with  $\text{CuK}\alpha$  radiation) and scanning electron microscopy (SEM, JEOL JSM-6360 LV), respectively.

The capacitive properties of as-obtained products were performed by cyclic voltammetry (CV) and chronopotentiometry with a CHI 660B electrochemical workstation in a three-electrode cell. The prepared film was employed as the working electrode. A Pt plate was used as the counter electrode and a saturated calomel electrode (SCE) as reference electrode. The experiments were operated at room temperature with  $2$  M KOH solution as electrolyte.

## RESULTS AND DISCUSSION

**XRD analyses:** Fig. 1 displays XRD patterns of  $\text{Co}(\text{OH})_2$  film (a),  $\text{Co}_3\text{O}_4$  film prepared by calcining  $\text{Co}(\text{OH})_2$  film at  $200$  °C (b) and  $300$  °C (c). As shown in curve a, the peaks are assigned to  $\text{Co}(\text{OH})_2$  (JCPDS No. 74-1057) and Ni substrate (JCPDS No. 87-0712). The peaks in curves b and c are indexed as  $\text{Co}_3\text{O}_4$  (JCPDS No. 73-1701) and Ni substrate (JCPDS No. 87-0712), indicating that  $\text{Co}_3\text{O}_4$  film has been formed by calcining  $\text{Co}(\text{OH})_2$  film at  $200$  and  $300$  °C. Besides, X-ray diffraction peaks of  $\text{Co}_3\text{O}_4$  strengthen and narrow when calcining temperature increases from  $200$ - $300$  °C. This demonstrates that crystallite sizes of  $\text{Co}_3\text{O}_4$  film calcined at  $300$  °C is larger than that of  $\text{Co}_3\text{O}_4$  film calcined at  $200$  °C. Similar phenomenon can be found in the reference<sup>24</sup>.

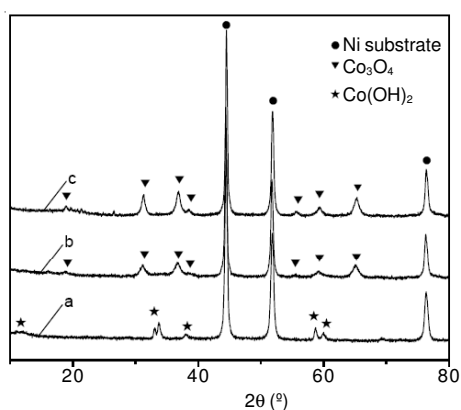
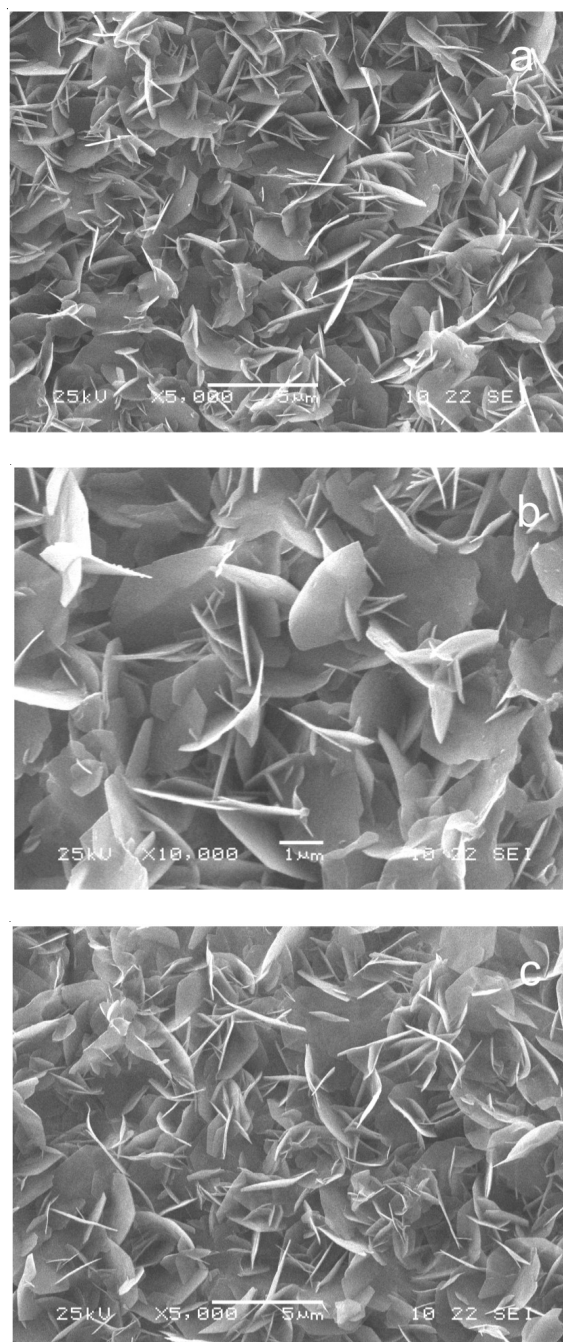


Fig. 1. XRD patterns of  $\text{Co}(\text{OH})_2$  film (a),  $\text{Co}_3\text{O}_4$  film prepared by calcining  $\text{Co}(\text{OH})_2$  film at  $200$  °C (b) and  $300$  °C (c)

**Morphology:** Fig. 2 shows SEM images of  $\text{Co}(\text{OH})_2$  film (a, b),  $\text{Co}_3\text{O}_4$  film prepared by calcining  $\text{Co}(\text{OH})_2$  film at  $200$  °C (c, d) and  $300$  °C (e, f). As shown in Fig. 2a-b, the morphology of electrodeposited  $\text{Co}(\text{OH})_2$  film consists of intercross nanoflakes with interspaces among them. It is evident that nanostructure of the entire  $\text{Co}(\text{OH})_2$  film is highly microporous. The average thickness of nanoflakes is about a few nanometers. As shown in Fig. 2c-f, the morphology of  $\text{Co}_3\text{O}_4$  film is consistent with that of  $\text{Co}(\text{OH})_2$  film, demonstrating that the surface morphology remains unchanged when  $\text{Co}(\text{OH})_2$  are converted into  $\text{Co}_3\text{O}_4$  by calcining. Moreover, change of heating temperature doesn't result in change of the morphology of film. The morphology of  $\text{Co}_3\text{O}_4$  film prepared by electrodeposition is different from that of  $\text{Co}_3\text{O}_4$  film prepared by a chemical bath<sup>22</sup>, which consists of spherical-like rough particles with some pores among particles.



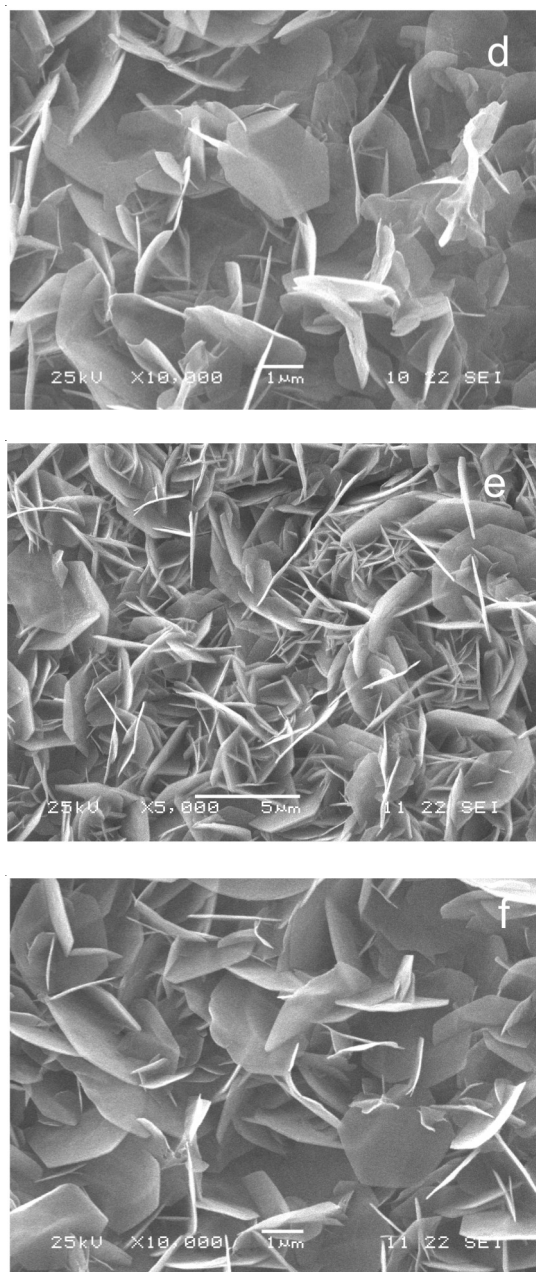


Fig. 2. SEM images of  $\text{Co(OH)}_2$  film (a, b),  $\text{Co}_3\text{O}_4$  film prepared by calcining  $\text{Co(OH)}_2$  film at 200 °C (c, d) and 300 °C (e, f): (a), (c) and (e): low magnification; (b), (d) and (f): high magnification

**Electrochemical properties:** Cyclic voltammograms of  $\text{Co(OH)}_2$  film are shown in Fig. 3. In reference<sup>9</sup>, there are two pairs of redox peaks in CV curves of  $\text{Co(OH)}_2$  film. As shown in Fig. 3, two pairs (denoted as  $\text{P}_1$ ,  $\text{P}_2$ ,  $\text{P}_3$  and  $\text{P}_4$ ) of redox peaks in CV curves of  $\text{Co(OH)}_2$  film should be observed. However, only  $\text{P}_1$ ,  $\text{P}_2$  and  $\text{P}_4$  are observed. This is because the  $\text{P}_3$  peaks exceed the potential range, namely  $\text{P}_3$  peak potential is higher than 0.5 V. The obvious redox peaks and the non-rectangular shape of CV curves reveal that the measured capacitance mainly results from the pseudo-capacitance, which is caused by faradaic redox reactions of electroactive material. Two redox peaks correspond to faradaic reactions as follows<sup>9</sup>:

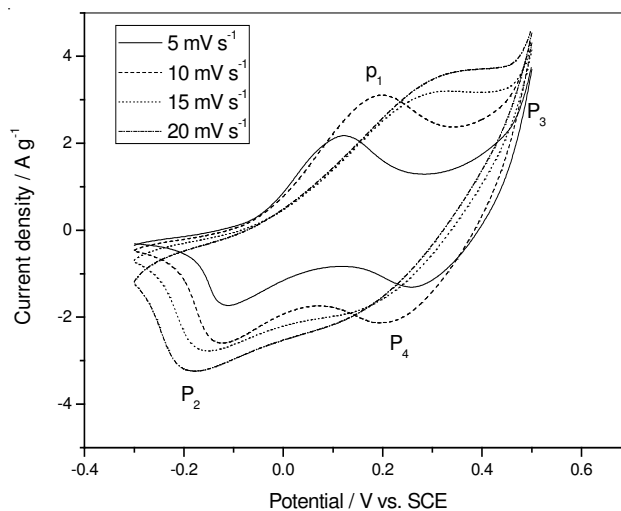
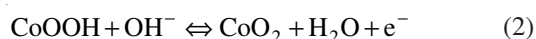


Fig. 3. Cyclic voltammograms of  $\text{Co(OH)}_2$  film at scan rates of 5, 10, 15 and 20  $\text{mV s}^{-1}$

Cyclic voltammograms of  $\text{Co}_3\text{O}_4$  film prepared by calcining  $\text{Co(OH)}_2$  film are demonstrated in Fig. 4. Similar CV curves are observed in the references<sup>22,25</sup>. The shape of CV curves is considerably different from an ideal rectangular shape, indicating that the measured capacitance mainly arises from pseudo-capacitance. A more elaborate discussion about electron transition and electrode reaction can be found in the references<sup>26,27</sup>. The faradaic redox reactions can be expressed as follows:

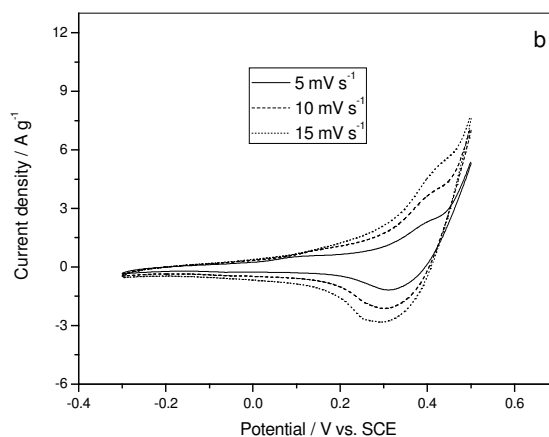
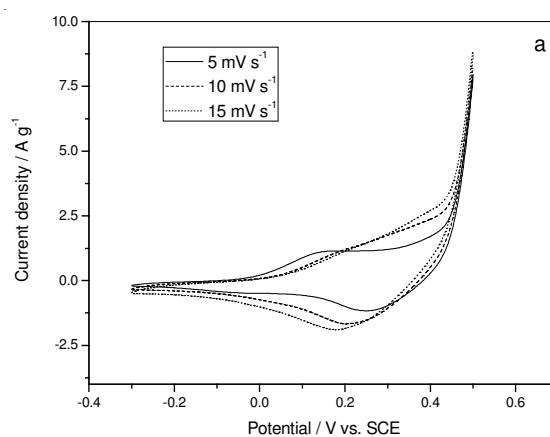


Fig. 4. Cyclic voltammograms of  $\text{Co}_3\text{O}_4$  film prepared by calcining  $\text{Co(OH)}_2$  film at scan rates of 5, 10 and 15  $\text{mV s}^{-1}$ . (a) 200 °C; (b) 300 °C

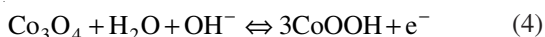
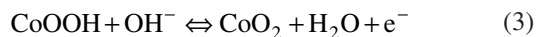


Fig. 5 displays cyclic voltammograms of Co(OH)<sub>2</sub> film and Co<sub>3</sub>O<sub>4</sub> film prepared by calcining Co(OH)<sub>2</sub> film at scan rates of 5 mV s<sup>-1</sup>. Compared with Co<sub>3</sub>O<sub>4</sub> film, Co(OH)<sub>2</sub> film shows the largest current density at the potential range -0.3~0.3 V, indicating that Co(OH)<sub>2</sub> film possesses the highest specific capacitance. Besides, Co<sub>3</sub>O<sub>4</sub> film prepared at 200 °C exhibits higher current density at the potential ranging from 0-0.3 V than that of Co<sub>3</sub>O<sub>4</sub> film prepared at 300 °C, indicating that Co<sub>3</sub>O<sub>4</sub> film prepared at 200 °C possesses higher specific capacitance than that of Co<sub>3</sub>O<sub>4</sub> film prepared at 300 °C.

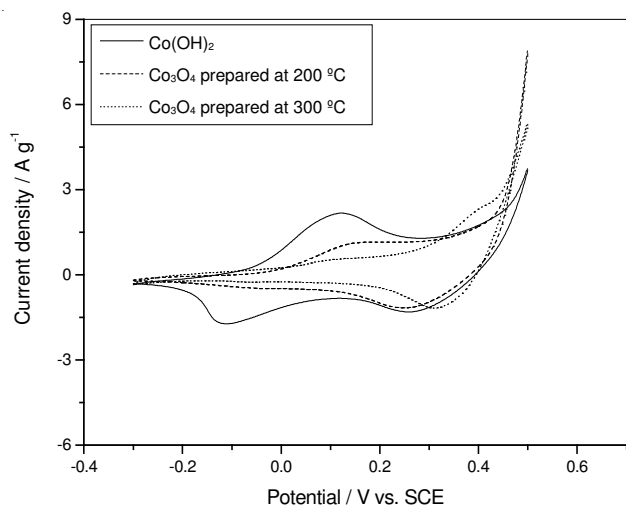


Fig. 5. Cyclic voltammograms of Co(OH)<sub>2</sub> film and Co<sub>3</sub>O<sub>4</sub> film prepared by calcining Co(OH)<sub>2</sub> film at scan rates of 5 mV s<sup>-1</sup>

Fig. 6 displays constant current discharge curves of Co(OH)<sub>2</sub> film and Co<sub>3</sub>O<sub>4</sub> film at different densities. The shape of discharge curves shows that a main pseudo-capacitance performance arises from the redox reaction occurred at an interface between the electrode and the electrolyte<sup>22,28</sup>. The result is in agreement with that from CV curves in Figs. 3 and 4. The specific capacitance ( $C_{sp}$ ) can be calculated from data shown in Fig. 5 by following the eqn. 5:

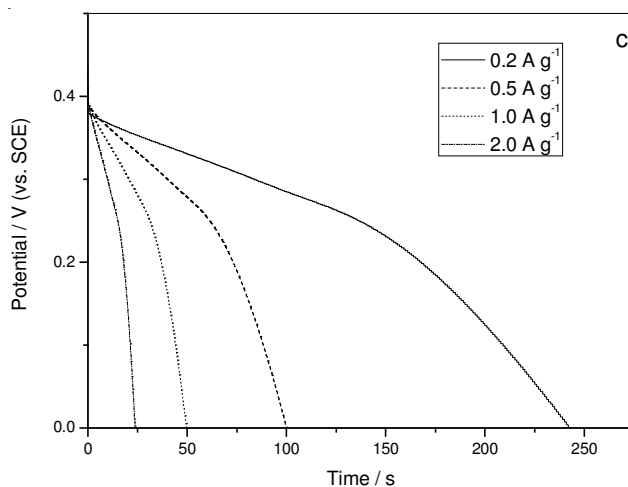
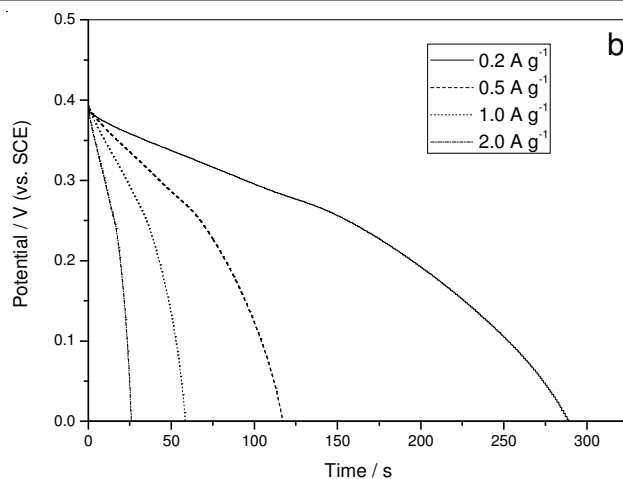
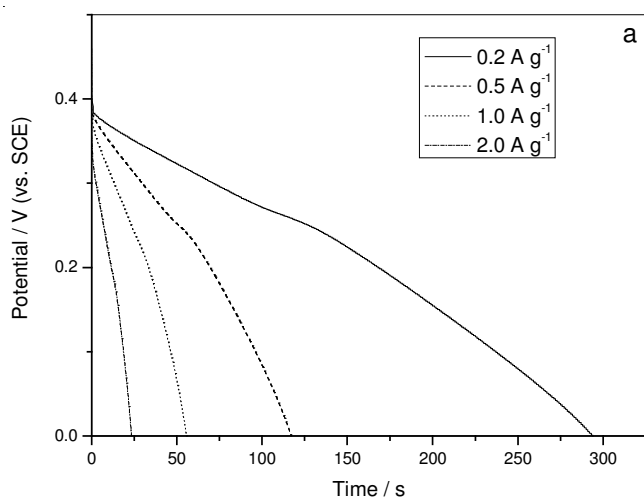


Fig. 6. Constant current discharge curves of electrode at different densities: (a) Co(OH)<sub>2</sub> film; (b) Co<sub>3</sub>O<sub>4</sub> film prepared by calcining Co(OH)<sub>2</sub> film at 200 °C; (c) Co<sub>3</sub>O<sub>4</sub> film prepared by calcining Co(OH)<sub>2</sub> film at 300 °C

$$C_{sp} = \frac{I \times t}{V \times m} \quad (5)$$

where  $I$ ,  $t$ ,  $V$  and  $m$  are the discharge current, the discharge time, potential difference during discharging and the mass of film, respectively. According to the equation above, the specific capacitance of three film electrodes at various current densities is shown in Fig. 7. It is noted that Co(OH)<sub>2</sub> film possesses higher specific capacitance at the same discharge current density than that of Co<sub>3</sub>O<sub>4</sub> film. This is ascribable to the fact that redox reaction process of Co(OH)<sub>2</sub> film occurred at film electrode/electrolyte interface is different from that of Co<sub>3</sub>O<sub>4</sub> film. The specific capacitance values of Co(OH)<sub>2</sub> film, Co<sub>3</sub>O<sub>4</sub> film prepared at 200 °C and Co<sub>3</sub>O<sub>4</sub> film prepared at 300 °C at the discharge current density of 0.2 A g<sup>-1</sup> are 153.4, 150.4 and 129.1 F g<sup>-1</sup>, respectively. In addition, Co<sub>3</sub>O<sub>4</sub> film prepared at 200 °C exhibits higher specific capacitance than that of Co<sub>3</sub>O<sub>4</sub> film prepared at 300 °C at the same discharge current density. This may be due to an increase in Co<sub>3</sub>O<sub>4</sub> crystallite size when calcining temperature increases from 200-300 °C. The increase in Co<sub>3</sub>O<sub>4</sub> crystallite size does not favor more active materials involved in redox reaction, thus causes its specific capacitance to reduce.

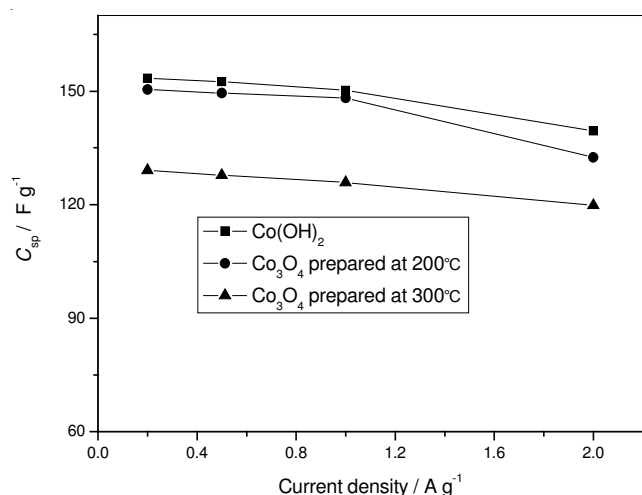


Fig. 7. Relationship between the specific capacitance and the current density of Co(OH)<sub>2</sub> film and Co<sub>3</sub>O<sub>4</sub> film

Fig. 8 shows that the specific capacitance retention ratio as a function of the current density. High specific capacitance retention ratio indicates that the electrode is suitable for high-rate charge-discharge. As shown in Fig. 8, the specific capacitance retention ratio of above 97 % is obtained in three film electrodes when the current density increases from 0.2-1.0 A g<sup>-1</sup>. The value is above 88 % at the current density range from 0.2-2.0 A g<sup>-1</sup>. These values are higher than those of our previous work about Co<sub>3</sub>O<sub>4</sub> film obtained by chemical bath deposition (67 %) <sup>22</sup>. The above results can be explained as follows. Compared with Co<sub>3</sub>O<sub>4</sub> film obtained by chemical bath deposition, Co<sub>3</sub>O<sub>4</sub> film prepared by electrochemical deposition exhibits different morphologies and structures, including crystal sizes, orientations and stacking manners <sup>29</sup>. The morphology of Co<sub>3</sub>O<sub>4</sub> film prepared by electrochemical deposition consists of intercross nanoflakes with interspaces among them. However, the morphology of spherical-like rough particles with some pores among particles is presented in Co<sub>3</sub>O<sub>4</sub> film prepared by chemical bath deposition. Morphology of Co<sub>3</sub>O<sub>4</sub> film prepared by electrochemical deposition is more advantageous to high-rate charge-discharge, resulting in the fact that its specific capacitance retention ratio is larger than that of Co<sub>3</sub>O<sub>4</sub> film prepared by chemical bath deposition.

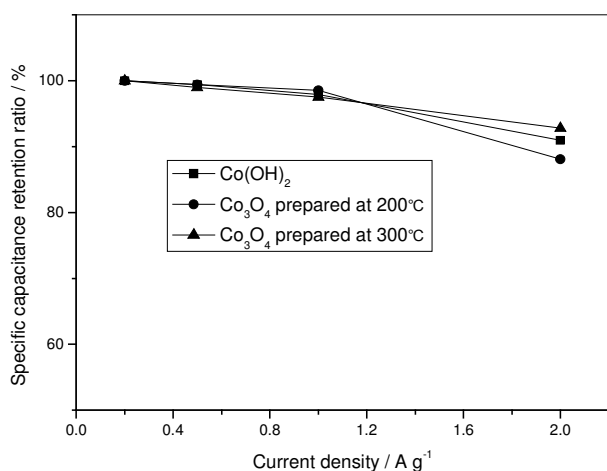


Fig. 8. Specific capacitance retention ratio as a function of the current density

## Conclusion

Co(OH)<sub>2</sub> film with intercross nanoflakes is prepared by electrodeposition and then Co<sub>3</sub>O<sub>4</sub> film with unchanged morphology is obtained by calcining Co(OH)<sub>2</sub> film. The results show that capacitive characteristic of Co(OH)<sub>2</sub> film and Co<sub>3</sub>O<sub>4</sub> film mainly results from pseudo-capacitance. At the current density of 0.2 A g<sup>-1</sup>, the specific capacitance of Co(OH)<sub>2</sub> film, Co<sub>3</sub>O<sub>4</sub> film obtained by calcining at 200 and 300 °C are 153.4, 150.4 and 129.1 F g<sup>-1</sup>, respectively. The specific capacitance retention ratio of three film electrodes is above 97 % at the current density range from 0.2-1.0 A g<sup>-1</sup> and reduces to above 88 % at the current density range from 0.2-2.0 A g<sup>-1</sup>. These values are higher than those of chemical bath deposited Co<sub>3</sub>O<sub>4</sub> film in previous work. This solves the problem of a relative lower specific capacitance retention ratio about Co<sub>3</sub>O<sub>4</sub> film prepared by a chemical bath.

## ACKNOWLEDGEMENTS

This work is supported financially by National Natural Science Foundation of China (No. 50972165), Scientific Research Fund of Hunan Provincial Education Department (No. 09C1055).

## REFERENCES

1. T. Zhao, H. Jiang and J. Ma, *J. Power Sources*, **196**, 860 (2011).
2. V. Ruiz, C. Blanco, E. Raymundo-Pinero, V. Khomenko, F. Beguin and R. Santamaria, *Electrochim. Acta*, **52**, 4969 (2007).
3. J. Li, X.Y. Wang, Y. Wang, Q.H. Huang, C.L. Dai, S. Gamboa and P.J. Sebastian, *J. Non-Cryst. Solids*, **354**, 19 (2008).
4. H. Pan, J.Y. Li and Y.P. Feng, *Nanoscale Res. Lett.*, **5**, 654 (2010).
5. R. Kavian, A. Vicenzo and M. Bestetti, *J. Mater. Sci.*, **46**, 1487 (2011).
6. Q.H. Huang, X.Y. Wang and J. Li, *Electrochim. Acta*, **52**, 1758 (2006).
7. J. Cheng, G.P. Cao and Y.S. Yang, *J. Power Sources*, **159**, 734 (2006).
8. W.J. Zhou, M.W. Xu, D.D. Zhao, C.L. Xu and H.L. Li, *Micropor. Mesopor. Mater.*, **117**, 55 (2009).
9. Z.A. Hu, Y.L. Xie, Y.X. Wang, L.J. Xie, G.R. Fu, X.Q. Jin, Z.Y. Zhang, Y.Y. Yang and H.Y. Wu, *J. Phys. Chem. C*, **113**, 12502 (2009).
10. R.K. Sharma, A.C. Rastogi and S.B. Desu, *Electrochim. Commun.*, **10**, 268 (2008).
11. S. Chen, J.W. Zhu and X. Wang, *J. Phys. Chem. C*, **114**, 11829 (2010).
12. W.Y. Li, S.Y. Zhang and J. Chen, *J. Phys. Chem. B*, **109**, 14025 (2005).
13. P. Elumalai, H.N. Vasan and N. Munichandraiah, *J. Power Sources*, **93**, 201 (2001).
14. V. Gupta, T. Kusahara, H. Toyama, S. Gupta and N. Miura, *Electrochim. Commun.*, **9**, 2315 (2007).
15. X.W. Lou, D. Deng, J.Y. Lee and L.A. Archer, *J. Mater. Chem.*, **18**, 4397 (2008).
16. K.M. Shaju, F. Jiao, A. Debart and P.G. Bruce, *Phys. Chem. Chem. Phys.*, **9**, 1837 (2007).
17. Y.H. Li, K.L. Huang, S.Q. Liu, Z.F. Yao and S.X. Zhuang, *J. Solid State Electrochem.*, **15**, 587 (2011).
18. Y.G. Zhang, Y.C. Chen, T. Wang, J.H. Zhou and Y.G. Zhao, *Micropor. Mesopor. Mater.*, **114**, 257 (2008).
19. X.H. Xia, J.P. Tu, J. Zhang, X.H. Huang, X.L. Wang, W.K. Zhang and H. Huang, *Electrochim. Commun.*, **10**, 1815 (2008).
20. T.C. Liu, W.G. Pell and B.E. Conway, *Electrochim. Acta*, **44**, 2829 (1999).
21. M.S. Wu, Y.A. Huang, C.H. Yang and J.J. Jow, *Int. J. Hydrogen Energy*, **32**, 4153 (2007).
22. Y.H. Li, K.L. Huang, Z.F. Yao, S.Q. Liu and X.X. Qing, *Electrochim. Acta*, **56**, 2140 (2011).
23. S.L. Chou, J.Z. Wang, H.K. Liu and S.X. Dou, *J. Power Sources*, **182**, 359 (2008).
24. L.B. Kong, J.J. Cai, L.L. Sun, J. Zhang, Y.C. Luo and L. Kang, *Mater. Chem. Phys.*, **122**, 368 (2010).
25. L. Cao, M. Lu and H.L. Li, *J. Electrochem. Soc.*, **152**, A871 (2005).
26. Z. Fan, J.H. Chen, K.Z. Cui, F. Sun, Y. Xu and Y.F. Kuang, *Electrochim. Acta*, **52**, 2959 (2007).
27. Y.H. Li and K.L. Huang, *Acta Chim. Sin.*, **69**, 2185 (2011).
28. Y.H. Li, K.L. Huang, D.M. Zeng, S.Q. Liu and Z.F. Yao, *J. Solid State Electrochem.*, **14**, 1205 (2010).
29. B.Y. Geng, F.M. Zhan, C.H. Fang and N. Yu, *J. Mater. Chem.*, **18**, 4977 (2008).